ORIGINAL ARTICLE

WILEY | Journal of **Food Processing and Preservation** | Institute of Food Science + Technology **ifst**

Modeling the rheological behavior of thermosonic extracted guava, pomelo, and soursop juice concentrates at different concentration and temperature using a new combination model

Norazlin Abdullah[1,2] 🄳 | **Nyuk L. Chin[2]** | **Yus A. Yusof[2]** | **Rosnita A. Talib[2]**

[1]Department of Technology and Heritage, Faculty of Science, Technology and Human Development, Universiti Tun Hussein Onn Malaysia (UTHM), Parit Raja, Batu Pahat, Johor, 86400, Malaysia

[2]Department of Process and Food Engineering Faculty of Engineering, Universiti Putra Malaysia, 43400 UPM, Serdang, Selangor, Malaysia

Correspondence
Nyuk L. Chin, Department of Process and Food Engineering, Faculty of Engineering, Universiti Putra Malaysia, 43400 UPM, Serdang, Selangor, Malaysia.
Email: chinnl@upm.edu.my

Abstract

This study has modeled the rheological behavior of thermosonic extracted pink-fleshed guava, pink-fleshed pomelo, and soursop juice concentrates at different concentrations and temperatures. The effects of concentration on consistency coefficient (K) and flow behavior index (n) of the fruit juice concentrates was modeled using a master curve which utilized the concentration-temperature shifting to allow a general prediction of rheological behaviors covering a wide concentration. For modeling the effects of temperature on K and n, the integration of two functions from the Arrhenius and logistic sigmoidal growth equations has provided a new model which gave better description of the properties. It also alleviated the problems of negative region when using the Arrhenius model alone. The fitted regression using this new model has improved coefficient of determination, R^2 values above 0.9792 as compared to using the Arrhenius and logistic sigmoidal models alone, which presented minimum R^2 of 0.6243 and 0.9440, respectively.

Practical applications

In general, juice concentrate is a better form of food for transportation, preservation, and ingredient. Models are necessary to predict the effects of processing factors such as concentration and temperature on the rheological behavior of juice concentrates. The modeling approach allows prediction of behaviors and determination of processing parameters. The master curve model introduced in this study simplifies and generalized rheological behavior of juice concentrates over a wide range of concentration when temperature factor is insignificant. The proposed new mathematical model from the combination of the Arrhenius and logistic sigmoidal growth models has improved and extended description of rheological properties of fruit juice concentrates. It also solved problems of negative values of consistency coefficient and flow behavior index prediction using existing model, the Arrhenius equation. These rheological data modeling provide good information for the juice processing and equipment manufacturing needs.

1 | INTRODUCTION

Fruit juice contains low-molecular-weight solutes such as sugars, organic acids, flavors, aromas, and vitamins, and high-molecular-weight solutes such as pectins, proteins, enzymes, and microorganisms (DasGupta & Sarkar, 2012; Sharoba & Ramadan, 2011). Its total soluble solids content is mainly constituted by the low-molecular-weight

sugars, giving it a sticky behavior and often referred for sweetness estimation in fruits and fruit-based products including fruit powders and juices (Jha & Gunasekaran, 2010; Pereira, Carvalho, Cabeça, & Colnago, 2013; Quek, Chok, & Swedlund, 2007). The total soluble solids content is also known to give rheological characteristics to fruit juices (Kaya & Sözer, 2005) where it plays an essential role in determining the magnitude of viscosity. Information on viscosities of concentrated fruit juice

is important to ensure it is pumpable and provides desired final product properties including the mouth feel properties for fruit juice.

Due to high water content in fruit juice, concentrating fruit juice in industrial processing is necessary to reduce packaging, storage, and transportation costs. Fruit juice concentrates are usually reconstituted at the time of usage by adding water. In producing juice concentrates, the water removal must be sufficient to increase its total soluble solids content until its °Brix level is at least 50% greater than its established reconstituted juice (Codex, 2005). Most food concentrates used in food industry are in the range of 30 to 40°Brix (Sharoba & Ramadan, 2011). Since fruit juice is a thermally sensitive product, concentrating by heating could develop a cooked taste in the final product and fouling in the pipe wall. The nutrient content in the fruit juice are also degraded by heat. These losses are serious processing and marketing problems. The freeze-drying process is introduced to concentrate fruit juice to produce the highest end product quality in terms of taste, aroma, nutritive value, and a longer shelf life. This process involves crystallization of water at low temperature and then sublimation from solid to vapor without passing through the liquid phase. In extracting heat-sensitive and starchy or creamy fruit juices, the use of thermosonic method has helped to increase juice yield at reduced heat levels (Abdullah, 2015; Chemat, Zill, & Khan, 2011).

Temperature is the most important control parameter in fruit juice processing because fruit juice concentrates are very heat-sensitive. Excessive heat and viscosity of fruit juice concentrates cause loss of energy and lower juice amount produced. Fruit juice may also overheat where less nutritious fruit juice is produced and its flavor and aroma degrade. The effect of temperature on rheological properties of fruit juices such as pomegranate and pear juice concentrates (Magerramov, Abdulagatov, Azizov, & Abdulagatov, 2007), untreated and pasteurized carrot juice (Vandresen, Quadri, de Souza, & Hotza, 2009), clarified pear and apple juices (Falguera, Vicente, Garvín, & Ibarz, 2013), and aloe vera juice concentrates (Swami Hulle, Patruni, & Rao, 2014) have been well described using the Arrhenius model. The Arrhenius model is based on temperature change, which causes thermal expansion by the magnitude of flow activation energy. The thermal energy results in the changes of intermolecular distances by the intermolecular forces (Vandresen et al., 2009). The flow activation energy is defined as sensitivity of sample viscosity to temperature changes (Juszczak, Witczak, Fortuna, & Solarz, 2014; Kaya & Sözer, 2005). The activation energy parameter in the Arrhenius model explains the minimum amount of energy that is enough for collision of molecules to initiate bonds breakage. Strong intermolecular forces and weak molecules mobility of the high viscosity fruit juices require a high amount of energy to be broken for starting the flow of fruit juices.

The aim of this study was to model rheological behavior of thermosonically extracted guava, pomelo, and soursop juice concentrates using the concentration-temperature superposition principle where a master curve is developed to display a single smooth line to express its rheological behavior. The present work has also developed and proposed a new mathematical model, which combines the Arrhenius and logistic growth models for modeling the effect of temperature on the rheological behavior of guava, pomelo, and soursop juice concentrates.

2 | MATERIALS AND METHODS

2.1 | Preparation of fruit juice concentrates

2.5 kg of each fruit pulp, the pink-fleshed guava (*Psidium guajava* L.), pink-fleshed pomelo (*Citrus maxima* M.), and soursop (*Annona muricata* L.) was blended in a commercial food blender (300 W, Model XB409, Ceado, Italy) at 28,000 rpm for 1 min, pulsed for 30 s and another 1 min at 22,000 rpm to get homogenized pulp. The pulp was then mixed with distilled water at ratio of 1:1 by weight before thermosonic treatment. Table 1 lists the conditions for thermosonic treatment for all three juices where it has been optimized priory for the highest juice yield with maximum ascorbic acid and total soluble solids content (Abdullah, 2015). Direct thermosonic treatment was carried out using a 400 W digital ultrasonic processor (S-450D, Branson Ultrasonics Corporation, Danbury, CT) with its probe tip immersed to a depth of 25 mm into a 150 mL beaker containing soursop pulp mixture. For indirect thermosonic treatment, a glass bottle of the guava or pomelo pulp mixture was partially immersed in an ultrasonic water bath (Chin, Tan, Che Pa, & Yusof, 2013), which contained water. The thermosonic treatment temperature was maintained using a temperature probe where cold water was added into the surrounding water of beaker containing sample for direct thermosonication or applying continuous flow of water into the bath for indirect thermosonication.

The thermosonic treated pulp mixture was centrifuged at 4,000 rpm for 20 min at 4 °C using a refrigerated centrifuge (Mikro 22R, Hettich Zentrifugen, Germany) to separate the fruit precipitate and liquid supernatant. The supernatant was collected as the thermosonic extracted juice and filled into plastic containers (100 mL), frozen in a freezer at −20 °C prior to freeze-drying. Ten containers of each frozen guava, pomelo, and soursop juice were concentrated in a freeze-dryer (FreeZone, Labconco) at vacuum pressure of 0.06 mbar for 72 hr where the average final concentration of guava, pomelo, and soursop juices produced were 47.8 ± 0.7°Brix, 73.1 ± 0.4°Brix, and 73.8 ± 0.7°Brix, respectively. The guava juice concentrate was diluted using distilled water to concentrations of 5, 15, 30, and 45°Brix, while the pomelo and soursop juice concentrates to concentrations of 5, 15, 30, 45, and 70°Brix for rheological measurements. Each concentrated juice was diluted in duplicate. The whole process of blending, homogenization, thermosonic treatment, concentration, and dilution of each fruit juice was repeated twice. The concentration was measured using a digital refractometer (PAL-Alpha, Atago) and expressed in °Brix.

TABLE 1 Optimized conditions for fruit juice extraction

| Factors | Optimum value | | |
	Guava Indirect thermosonication	Pomelo Indirect thermosonication	Soursop Direct thermosonication
Intensity[a]	1	2.5	10
Time (min)	30	23	10
Temperature (°C)	55	54	55

[a]Intensity in amplitude (%) for direct thermosonication and in power (kW) for indirect thermosonication.

2.2 | Rheological measurements

The rheological properties were measured using a rheometer (ARG2, TA Instruments) with the 40-mm cone and diameter plate geometry for shear rate range of 0–400 s^{-1}. Steady-state flow test was conducted for each juice concentrate samples at temperatures of 0, 4, 10, 25, 40, 60, and 80°C. Shear stress versus shear rate data were fitted to the power law model (Equation 1) to obtain values of consistency coefficient (K) and flow behavior index (n) in studying the flow behavior of the juice concentrates. Its viscosity (η) is reported as a function of shear rate (Equation 1a) (Steffe, 1996).

$$\sigma = K\dot{\gamma}^n \tag{1}$$

$$\eta = K(\dot{\gamma})^{n-1} \tag{1a}$$

where, σ is the shear stress (Pa), K is the consistency coefficient, $\dot{\gamma}$ is the shear rate (s^{-1}), and n is the flow behavior index.

2.3 | Modeling the effect of concentration on the juice concentrates flow behavior

The effect of concentration (C) on the variation of K or n can be described by the exponential (Equations 2a and 2b) and power law (Equations 3a and 3b) models. The exponential (Dak, Verma, & Jaaffrey, 2007; Yilmaz, Sert, & Demir, 2010) and power law (Barbana & El-Omri, 2012; Dak et al., 2007; Yilmaz et al., 2010) are the most widely fitted empirical models for predicting values of K and n.

$$K = k_c \exp(bC) \tag{2a}$$

$$n = n_c \exp(bC) \tag{2b}$$

$$K = k_c C^b \tag{3a}$$

$$n = n_c C^b \tag{3b}$$

where k_c, n_c, and b is the constants and C is the concentration.

The dimensionless concentration-temperature shift factors, a_T at each temperature were calculated using Equation 4 to make a horizontal shift of other temperatures at the concentration axis to make an overlapped smooth curve. 25°C was chosen as the reference temperature (Quek, Chin, & Yusof, 2013).

$$a_T = C_T / C_{T_{ref}} \tag{4}$$

where a_T is the dimensionless shift factor, C_T is the concentration at defined temperature, and C_{Tref} is the concentration at reference temperature of 25°C.

A master curve was then plotted as K or n versus C/a_T where exponential model (Equations 5a and 5b) or power law model (Equations 6a and 6b) was fitted to find the best regressed master curve model for each fruit concentrate.

$$K = k_c' \exp\left[b'\left(\frac{C}{a_T}\right)\right] \tag{5a}$$

$$n = n_c' \exp\left[b'\left(\frac{C}{a_T}\right)\right] \tag{5b}$$

$$K = k_c'\left(\frac{C}{a_T}\right)^{b'} \tag{6a}$$

$$n = n_c'\left(\frac{C}{a_T}\right)^{b'} \tag{6b}$$

where k_c', n_c', and b' are the constants, K is the consistency coefficient, n is the flow behavior index, C is the concentration, and a_T is the dimensionless shift factor.

2.4 | Modeling the effect of temperature on the juice concentrates flow behavior

The variation of K or n as function temperature was modeled using the Arrhenius model in Equations 7a and 7b, logistic sigmoidal growth model (Augusto, Soares, Chiu, & Gonçalves, 2012) in Equations 8a and 8b, and also the proposed new model in Equations 9a and 9b. The original logistic sigmoidal model, $dN/dt = rN(1-N/H)$ is based on approximation of population growth in the United States, where N is the number of population, t is the time, r is the growth parameter, and H is the carrying capacity (Pearl & Reed, 1920). The equation is integrated to get logistic model as in Equation 8a. The separable of variable method, $\int dN/[N(1-N/H)] = \int r\ dt$ is applied to the original logistic sigmoidal model prior to the integration step to bring together N variable on left side and t variable on right side. The integration gives $\ln\{D[N(t)]/[H-N(t)]\} = rt$. All terms at both sides of this integrated equation were then exponent to eliminate the logarithm term, which is written as $\{D[N(t)]\}/\{[H-N(t)]\} = \exp(rt)$. By rearranging and adding fractions into the equation, a sigmoidal growth model $N(t) = H/[D\exp(-rt)+1]$ with positive value of r is obtained. In this study, N as function of time is replaced with K as function of temperature and decay function is suitable to be used because K reduces by temperature increment. Therefore, r is a negative value to make it a decay function and logistic sigmoidal models for this study are as in Equations 8a and 8b. Cross product of the Arrhenius (Equations 7a and 7b) and logistic sigmoidal growth (Equations 8a and 8b) models yields the proposed new model as in Equations 9a and 9b.

$$K = k_T \exp\left(-\frac{E_a}{RT}\right) \tag{7a}$$

$$n = n_T \exp\left(-\frac{E_a}{RT}\right) \tag{7b}$$

$$K(T) = \frac{H}{D\exp(-rT)+1} \tag{8a}$$

$$n(T) = \frac{H}{\exp(-rT)} \tag{8b}$$

$$K = \frac{Hk_T \exp\left(\frac{E_a}{RT}\right)}{D\exp(-rT)+1} \tag{9a}$$

$$n = \frac{Hn_T \exp\left(\frac{E_a}{RT}\right)}{D\exp(-rT)+1} \tag{9b}$$

where K is the consistency coefficient, n is the flow behavior index, T is temperature in Kelvin, k_T and n_T are the pre-exponential factor, E_a is the activation energy in kJ mol^{-1}, R is the universal gas constant of 8.314 J mol^{-1} K^{-1}, H is the maximum value of the asymptotic curve, k_T, n_T, and D are constants and r is the growth parameter.
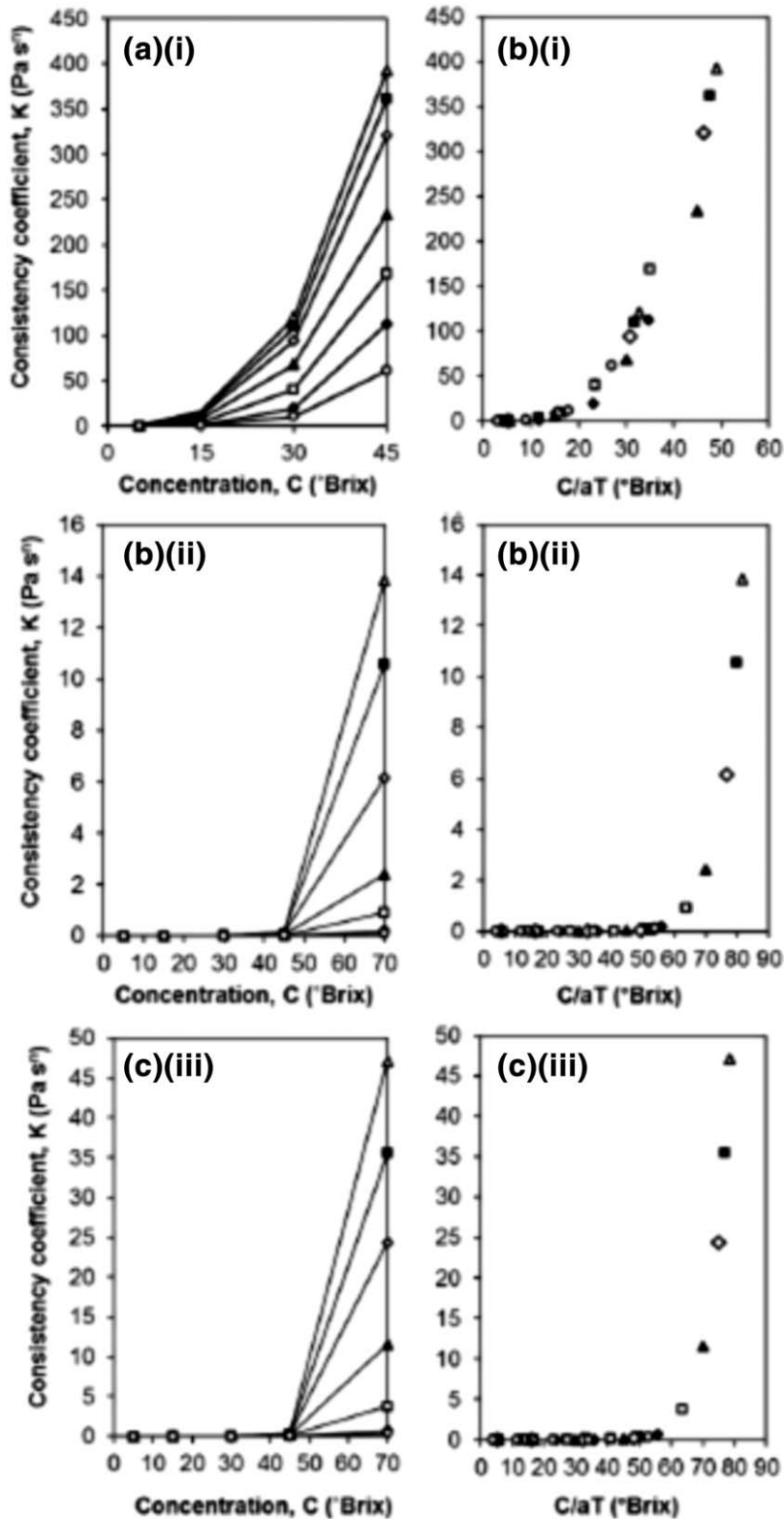
FIGURE 1 Effect of concentration on consistency coefficient, K of (a)(i) guava, (b)(i) pomelo, and (c)(i) soursop at temperatures of 0 °C (Δ), 4 °C (■), 10 °C (¤), 25 °C (▲), 40 °C (□), 60 °C (◆), and 80 °C (○) and their respective master curve (a)(ii), (b)(ii), and (c)(ii)

2.5 | Statistical analysis

The coefficient of determination, $R^2 = 1 - \text{SSE/SST} = \sum \left(y_{\text{experimental}} - y_{\text{model}}\right)^2 / \sum \left(y_{\text{experimental}} - \bar{y}_{\text{experimental}}\right)^2$ was determined for each temperature or the master curve in choosing the best fitted model, where SSE is the sum of square error, SST is the total sum of squares, $y_{\text{experimental}}$ is the experimental value of dependent variable, y_{model} is the model value of dependent variable, and $\bar{y}_{\text{experimental}}$ is the mean of experimental value of dependent variable. Curve fitting was
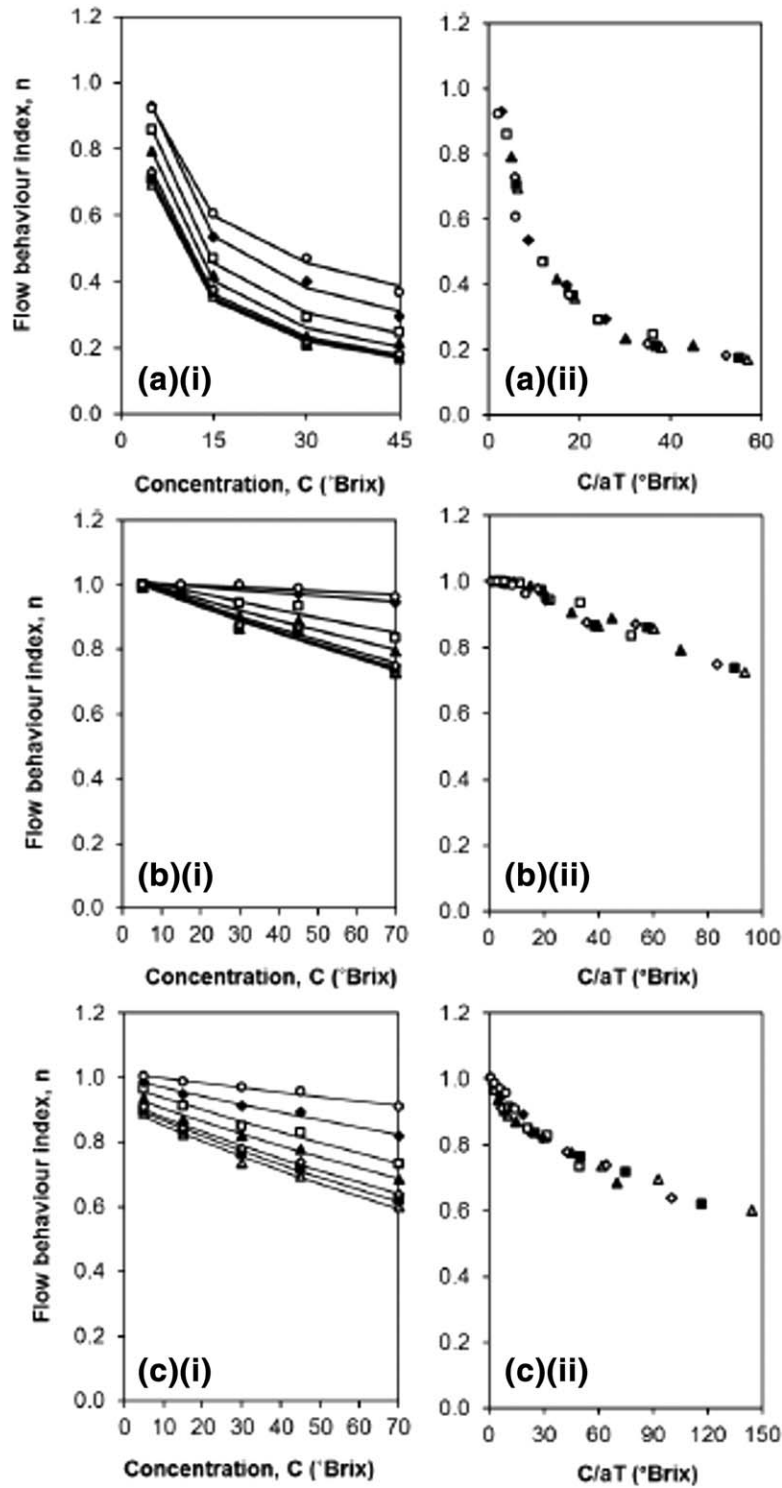
FIGURE 2 Effect of concentration on flow behavior index of (a)(i) guava, (b)(i) pomelo, and (c)(i) soursop at temperatures of 0 °C (△), 4 °C (■), 10 °C (¤), 25 °C (▲), 40 °C (□), 60 °C (◆), and 80 °C (○) and their respective master curve (a)(ii), (b)(ii), and (c)(ii)

done using the solver function in Microsoft Excel 2007 (XP Edition, Microsoft Corporation). Root mean square error, RMSE$=\sqrt{\left[\sum_{i=1}^{N}\left(y_{\text{experimental},i}-y_{\text{model},i}\right)^2\right]/N}$ was used to assess the variation in dependent variable that the model did not explain, where N is the number of data. The highest R^2 and the lowest $RMSE$ values determined the best fitted model. The goodness of model fitting was also

determined by a plot of the model values of K or n (y_{model}) versus the experimental values of K or n($y_{\text{experimental}}$) as $y_{\text{model}}=V \cdot y_{\text{experimental}}-W$, where V is the line slope, and W is the y_{model}-intercept. A straight line with slope (V) value near to one, y_{model}-intercept (W) near to zero and R^2 near to one was considered as the best fitted model (Augusto, Falguera, Cristianini, & Ibarz, 2012). The analysis and comparison of

TABLE 2 Constant values for exponential and power law models of K as a function of concentration for guava, pomelo and soursop juice concentrates

T (°C)	Guava				Pomelo				Soursop			
	k_T	b	R^2	RMSE	k_T	b	R^2	RMSE	k_T	b	R^2	RMSE
Exponential												
0	7.8743E+00	0.0870	0.9932	0.0348	5.6226E−05	0.1773	1.0000	0.0348	6.2094E−05	0.1934	1.0000	0.0386
4	6.9921E+00	0.0878	0.9936	0.0287	5.3008E−05	0.1743	1.0000	0.0287	9.7100E−05	0.1830	1.0000	0.0381
10	5.8169E+00	0.0892	0.9944	0.0204	5.9378E−05	0.1650	0.9999	0.0204	9.4820E−05	0.1779	1.0000	0.0271
25	4.0977E+00	0.0900	0.9943	0.0081	3.6785E−05	0.1584	0.9999	0.0081	4.9108E−05	0.1767	1.0000	0.0086
40	1.7859E+00	0.1010	0.9976	0.0022	1.5952E−05	0.1565	1.0000	0.0022	4.8858E−05	0.1608	1.0000	0.0048
60	5.1655E−01	0.1196	0.9995	0.0023	3.4280E−06	0.1565	0.9991	0.0023	6.2014E−06	0.1663	0.9989	0.0091
80	3.2653E−01	0.1164	0.9991	0.0024	2.0120E−06	0.1565	0.9973	0.0024	3.4577E−06	0.1649	0.9986	0.0053
Power law												
0	5.2855E−03	2.9462	0.9997	2.6278	5.9803E−07	3.9846	0.9653	1.0297	4.7335E−07	4.3298	0.9756	2.9382
4	4.2626E−03	2.9810	0.9998	2.2829	7.5236E−07	3.8624	0.9611	0.8319	1.2652E−06	4.0284	0.9673	2.5610
10	2.9706E−03	3.0446	0.9998	1.6286	3.5441E−07	3.9135	0.9638	0.4673	5.3083E−07	4.1400	0.9702	1.6766
25	1.9229E−03	3.0759	0.9998	1.3890	1.1006E−06	3.4202	0.9440	0.2272	3.6613E−07	4.0547	0.9692	0.8061
40	2.2591E−04	3.5514	1.0000	0.2835	6.4398E−07	3.3066	0.9355	0.0923	3.7044E−07	3.7865	0.9631	0.2882
60	4.6198E−06	4.4684	0.9998	0.5722	2.5524E−07	3.1771	0.9467	0.0179	1.3653E−07	3.6292	0.9673	0.0503
80	2.6941E−06	4.4515	0.9995	0.5712	9.9695E−07	2.7224	0.9244	0.0124	1.1254E−07	3.5125	0.9647	0.0264

significant difference between temperatures (Figures 1 and 2) or concentrations (Figures 4 and 5) were analyzed using one-way analysis of variance (ANOVA) and Duncan's multiple range tests (DMRT) with statistical analysis software (SAS 9.2, SAS Institute, Inc.).

3 | RESULTS AND DISCUSSION

3.1 | Modeling the effect of concentration on flow behavior of juice concentrates

Figure 1 illustrates the effect of concentration on consistency coefficient, K at seven different temperatures ranging from 0 to 80°C. Generally, guava juice concentrates are thicker and has the widest range of K while the pomelo juice concentrates are most watery and has the lowest K

values. The value of high K at high concentration is attributed to the formation of a highly viscous gel-type layer on the membrane surface by pectin (Sharoba & Ramadan, 2011). Based on graphical and statistical analysis (Table 2), it was found that the power law model (Equation 3a) fitted better for the guava juice concentrates ($R^2 = 0.9995-1.0$; RMSE $= 0.2835-2.6278$) as compared to the exponential model ($R^2 = 0.9932-0.9995$; RMSE $= 0.7454-13.0210$). However, the exponential model (Equation 2a) is better fitted for pomelo ($R^2 = 0.9973-1.0$; RMSE $= 0.0022-0.0348$) and soursop juice concentrates ($R^2 = 0.9986-1.0$; RMSE $= 0.0048-0.0386$) as the power law model fit was poorer for pomelo ($R^2 = 0.9244-0.9653$; RMSE $= 0.0124-1.0297$) and soursop ($R^2 = 0.9631-0.9756$; RMSE $= 0.0264-2.9382$). ANOVA results show that the means of K for all three juices at temperatures range of 0 to 80°C have no significant difference as large p values of .3302, .2343, and .2769, respectively, for guava, pomelo, and soursop

TABLE 3 Constant values for exponential and power law models of n as a function of concentration for guava, pomelo, and soursop juice concentrates

T (°C)	Guava				Pomelo				Soursop			
	n_C	b	R^2	RMSE	n_C	b	R^2	RMSE	n_C	b	R^2	RMSE
Exponential												
0	0.8382	−0.0462	0.9492	0.0467	1.0246	−0.0047	0.9627	0.0184	0.9043	−0.0060	0.9879	0.0110
4	0.8515	−0.0459	0.9491	0.0474	1.0255	−0.0046	0.9583	0.0190	0.9160	−0.0057	0.9944	0.0073
10	0.8794	−0.0459	0.9453	0.0508	1.0284	−0.0044	0.9576	0.0185	0.9232	−0.0053	0.9911	0.0087
25	0.9448	−0.0442	0.9384	0.0576	1.0254	−0.0036	0.9683	0.0133	0.9466	−0.0046	0.9924	0.0074
40	0.9969	−0.0397	0.9378	0.0602	1.0265	−0.0027	0.9327	0.0154	0.9756	−0.0041	0.9816	0.0107
60	1.0358	−0.0326	0.9325	0.0628	1.0121	−0.0009	0.8959	0.0070	0.9947	−0.0027	0.9838	0.0072
80	0.9913	−0.0247	0.9420	0.0502	1.0095	−0.0006	0.8238	0.0061	1.0116	−0.0014	0.9768	0.0049
Power law												
0	1.9630	−0.6430	0.9979	0.0096	1.2079	−0.1010	0.8121	0.0413	1.1298	−0.1328	0.9227	0.0278
4	1.9867	−0.6399	0.9973	0.0109	1.2057	−0.0988	0.8183	0.0397	1.1271	−0.1243	0.9071	0.0295
10	2.0545	−0.6402	0.9977	0.0103	1.1988	−0.0938	0.8090	0.0392	1.1226	−0.1165	0.9082	0.0279
25	2.1647	−0.6222	0.9951	0.0163	1.1633	−0.0769	0.8097	0.0326	1.1239	−0.1021	0.8983	0.0270
40	2.1810	−0.5769	0.9983	0.0100	1.1215	−0.0559	0.7057	0.0322	1.1377	−0.0909	0.8909	0.0260
60	2.0867	−0.5005	0.9973	0.0125	1.0416	−0.0187	0.6156	0.0135	1.1034	−0.0610	0.8755	0.0198
80	1.7507	−0.3959	0.9965	0.0124	1.0262	−0.0112	0.5114	0.0101	1.0672	−0.0321	0.8068	0.0142

TABLE 4 Best fitted master curve models for k or n as a function of concentration for guava, pomelo and soursop juice concentrates

Fruit juice	Effect of C on K		Effect of C on n	
	Equation	R^2	Equation	R^2
Guava	$K = 0.0020 \left(\frac{C}{a_T} \right)^{3.1230}$	0.9836	$n = 1.5326 \left(\frac{C}{a_T} \right)^{-0.4912}$	0.9453
Pomelo	$K = 2.298 \times 10^{-5} \exp\left[0.1631 \left(\frac{C}{a_T} \right) \right]$	0.9993	$n = 1.0197 \exp\left[-0.0035 \left(\frac{C}{a_T} \right) \right]$	0.9647
Soursop	$K = 1.802 \times 10^{-5} \exp\left[0.1886 \left(\frac{C}{a_T} \right) \right]$	0.9982	$n = 0.9534 \exp\left[-0.0040 \left(\frac{C}{a_T} \right) \right]$	0.9324

were obtained. This supports the approach of consolidating the K values from different temperatures into a single line in the form of a master curve.

Figure 2 shows the relationship of n and C, which was also fitted to the exponential and power law models. The fruit juice concentrates tend to be more shear-thinning when concentrations increased. The guava juice concentrates have a more prominent shear thinning behavior than the pomelo and soursop. This is due to low starch content in guava, around 13% (Chek Zaini, Zaiton, Zanariah, & Sakinah, 2012) as compared to 27.3% starch content in soursop (Nwokocha & Williams, 2009). Non-starchy (Economos & Clay, 1999) and low pulp content causes the pomelo fruit is close to Newtonian behavior. Table 3 shows that the power law model (Equation 3b) was best fitted for guava juice concentrate with R^2 values between 0.9951 and 0.9983. The n for pomelo and soursop juice concentrates fitted the exponential model (Equation 2b) well with R^2 values of 0.8238−0.9683 for pomelo and 0.9768−0.9944 for the soursop. The ANOVA results indicate that means of n for pomelo and soursop with different temperature levels were significantly different with $p = .0046$ and $p < .0001$, respectively. However, means of n for guava was not significantly different with $p = .3342$. The DMRT results for pomelo and soursop shows that the average n at 80 °C was higher than n at 0 °C, thus suggest that shear-thinning behavior more prominent at lower temperature.

Figures 1a(ii),b(ii),c(ii) show a well superimposed smooth curve when K values are plotted against C/a_T. By fitting Equations 5a or 6a, the master curve can be used to predict the K at for its

respective concentration range for each juice concentrate. Figures 2a(ii),b(ii),c(ii) show the master curve for n for guava, pomelo, and soursop, respectively, suitable to be modeled using either Equations 5b or 6b for n prediction purposes. Table 4 lists the best fitted master curve models for K and n with their constants selected by the highest R^2 and lowest $RMSE$ values. These master curve models have acceptable R^2 values of more than 0.93, and can be used for predicting rheological properties, K and n of respective fruit juice concentrates. The negative constants suggest the decrement of n with increment of concentration.

Figure 3 shows the relationship of viscosity (Equation 1a) with concentration and shear rate. Viscosity is higher at lower shear rates because due to higher forces in breaking agglomerated molecules (Genovese & Lozano, 2001). The aggregation between molecules is attributed to pectinaceous substances, which have a high water holding capacity that develops a cohesive network structure (Bhattacharya & Rastogi, 1998). Lower viscosity is low at high shear rate was due to the molecules orientation and alignment, which reduced friction between molecules (Sun-Waterhouse, Bekkour, Wadhwa, & Waterhouse, 2014). The reduction in juice viscosities gives benefit to the high-shear processes like pumping and filling. Increase in viscosity with concentration is due to the increment of hydrated molecules and hydrogen bonding with the hydroxyl groups (Sharma, Manikantan, Ranote, & Singh, 2014). Cell wall debris such as cellulose and pectin which is usually made up by small amounts of hemicelluloses and hydroxyproline-rich protein may also be the main interference for juice to flow (Sharoba & Ramadan,
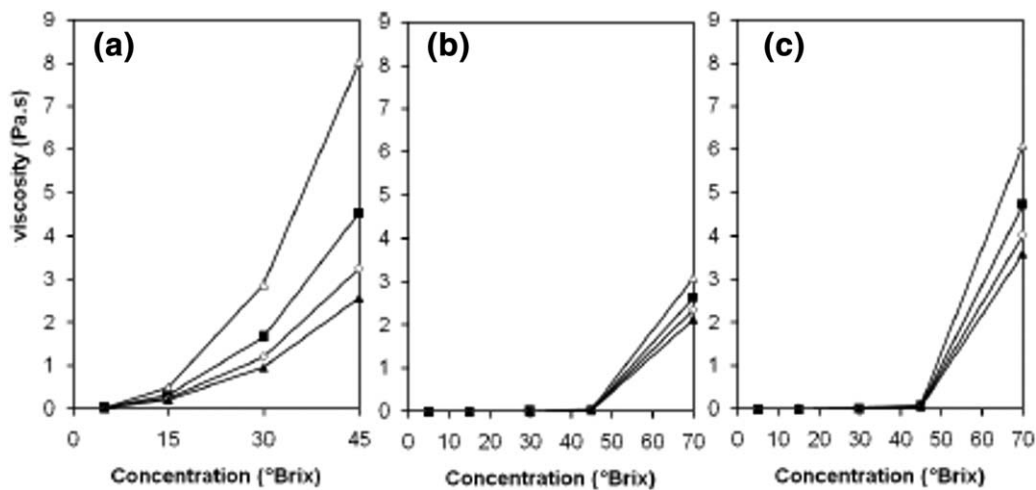

FIGURE 3 Effect of concentration on viscosity of (a) guava, (b) pomelo, and (c) soursop at shear rates of 100 s^{-1} (Δ), 200 s^{-1} (■), 300 s^{-1} (✣), and 400 s^{-1} (▲) at temperature of 4 °C

TABLE 5 Constant values for logistic sigmoidal decay and Arrhenius models of K as a function of temperature for guava, pomelo, and soursop

C (°Brix)	Arrhenius model				Logistic sigmoidal model					New model						
	k_T	E_a (kJ/mol)	R^2	RMSE	H	D	r	R^2	RMSE	k_T	E_a (kJ/mol)	H	D	r	R^2	RMSE
Guava																
5	1.36E−05	20.9688	0.9333	0.0145	0.7272	6.65E−06	−0.0485	0.9956	0.0037	1.8387	1.49E−03	1.3216	5.77E−05	−0.2248	0.9967	0.0032
15	1.04E−03	20.9688	0.9829	0.4835	15.1947	2.47E−07	−0.0530	0.9979	0.1698	0.6114	3.23E−05	11.9260	2.44E−06	−0.0475	0.9989	0.1228
30	1.87E−02	19.9981	0.9854	4.9051	152.1947	1.00E−07	−0.0546	0.9927	3.4679	0.6114	3.23E−05	121.9260	1.85E−06	−0.0475	0.9963	2.4568
45	2.72E−01	16.5741	0.9918	10.6811	392.1947	2.55E−08	−0.0562	0.9518	25.8999	0.5351	3.98E−05	390.1490	3.98E−05	−0.0372	0.9951	8.2749
70	NA	NA	NA	NA	NA	NA	NA	NA	NA	NA	NA	NA	NA	NA	NA	NA
Pomelo																
5	5.89E−08	23.9660	0.9133	0.0002	0.0442	3.18E−02	−0.0237	0.9850	0.0001	0.4395	4.83E−04	0.0023	1.09E−03	−0.0805	0.9972	0.0001
15	1.16E−07	23.9660	0.9512	0.0003	0.0726	6.79E−03	−0.0285	0.9743	0.0002	0.4395	4.61E−04	0.0048	2.64E−04	−0.0831	0.9941	0.0002
30	5.71E−07	23.9660	0.9923	0.0007	0.1967	1.03E−04	−0.0412	0.9933	0.0006	0.4494	4.17E−04	0.0985	5.57E−05	−0.0885	0.9982	0.0006
45	2.16E−06	23.9660	0.9798	0.0043	0.3846	6.56E−06	−0.0482	0.9912	0.0028	0.4496	4.14E−04	0.0993	1.25E−05	−0.0888	0.9969	0.0028
70	2.48E−06	35.1158	0.9716	0.8565	88.7895	7.58E−07	−0.0581	0.9745	0.8111	0.6545	3.98E−04	0.4322	2.21E−10	−0.1151	0.9978	0.3301
Soursop																
5	5.50E−06	15.0866	0.9180	0.0005	0.0166	6.05E−05	−0.0390	0.9899	0.0002	0.5751	1.57E−04	0.0082	1.33E−04	−0.0516	0.9982	0.0001
15	2.22E−05	15.0866	0.8813	0.0023	0.0449	2.66E−06	−0.0480	0.9763	0.0010	0.5752	1.49E−04	0.0213	1.93E−05	−0.0559	0.9954	0.0008
30	2.20E−05	18.5044	0.8498	0.0125	0.2246	1.07E−07	−0.0605	0.9440	0.0076	76.1748	2.36E−03	0.1024	2.85E−05	−0.3385	0.9863	0.0058
45	1.15E−05	23.4928	0.9641	0.0257	0.8225	8.05E−08	−0.0606	0.9783	0.0200	76.2029	5.25E−03	0.4694	4.77E−04	−0.6760	0.9959	0.0138
70	1.07E−05	34.6312	0.9891	1.7854	85.8225	3.87E−11	−0.0876	0.9893	1.7682	76.2275	1.20E−02	47.5090	1.30E−05	−1.5036	0.9984	0.9695

TABLE 6 Constant values for logistic sigmoidal decay and Arrhenius models of n as a function of temperature for guava, pomelo, and soursop

| C (°Brix)	Arrhenius model				Logistic sigmoidal model					New model						
	n_T	E_a (kJ/mol)	R^2	RMSE	H	D	r	R^2	RMSE	n_T	E_a (kJ/mol)	H	D	r	R^2	RMSE
Guava																
5	2.7602	−3.1072	0.9485	0.0211	0.9882	622.8684	0.0265	0.9801	0.0131	7.4796	−6.13E−05	2.7325	622.8293	0.0196	0.9889	0.0098
15	3.8095	−5.4251	0.9953	0.0060	0.6765	622.8678	0.0236	0.9709	0.0149	7.5048	−4.88E−05	2.8015	622.8290	0.0148	0.9980	0.0039
30	10.3649	−9.1147	0.9704	0.0166	0.8361	622.8678	0.0189	0.9690	0.0170	6.6279	−7.57E−06	0.5521	622.8378	0.0139	0.9792	0.0140
45	5.4894	−8.0105	0.9892	0.0071	0.5145	622.8679	0.0205	0.9781	0.0101	6.9120	−1.94E−05	0.7182	622.8293	0.0137	0.9965	0.0041
70	NA	NA	NA	NA	NA	NA	NA	NA	NA	NA	NA	NA	NA	NA	NA	NA
Pomelo																
5	1.0186	−0.0510	0.6243	0.0014	0.9998	2.76E+14	0.1403	0.9707	0.0004	23.5207	−8.10E−05	24.0201	622.3997	0.0102	1.0000	0.0013
15	1.1177	−0.3148	0.9329	0.0029	1.0029	2.74E+02	0.0329	0.9968	0.0006	20.6736	−9.37E−05	21.0611	622.4389	0.0126	1.0000	0.0010
30	1.7657	−1.6354	0.9696	0.0095	1.0965	1.43E+01	0.0144	0.9706	0.0093	13.6866	−8.73E−05	14.4324	622.6138	0.0144	0.9999	0.0084
45	1.6910	−1.5577	0.9849	0.0062	1.0706	1.43E+01	0.0146	0.9808	0.0070	14.9523	−8.38E−05	15.6423	622.5805	0.0133	1.0000	0.0058
70	2.7449	−3.0456	0.9738	0.0147	1.3574	1.44E+01	0.0102	0.9745	0.0145	9.5708	−7.23E−05	10.9132	622.6754	0.0143	0.9997	0.0140
Soursop																
5	1.5314	−1.2258	0.9911	0.0039	1.0840	7.2134	0.0128	0.9968	0.0023	14.1621	−9.27E−05	15.4068	622.6452	0.0149	1.0000	0.0026
15	1.8262	−1.8131	0.9960	0.0036	1.1588	7.2164	0.0105	0.9944	0.0043	14.1585	−7.84E−05	15.4034	622.6452	0.0127	1.0000	0.0032
30	2.3499	−2.6147	0.9925	0.0068	1.2431	12.1015	0.0106	0.9916	0.0072	12.0438	−6.53E−05	13.4684	622.6689	0.0119	0.9999	0.0066
45	2.7729	−3.1356	0.9978	0.0042	1.5324	12.1395	0.0085	0.9984	0.0037	11.0672	−4.99E−05	12.5982	622.6794	0.0103	1.0000	0.0046
70	3.5904	−4.0781	0.9910	0.0099	3.0077	25.2188	0.0067	0.9976	0.0052	6.6087	−6.11E−05	8.6358	622.7100	0.0145	0.9999	0.0088
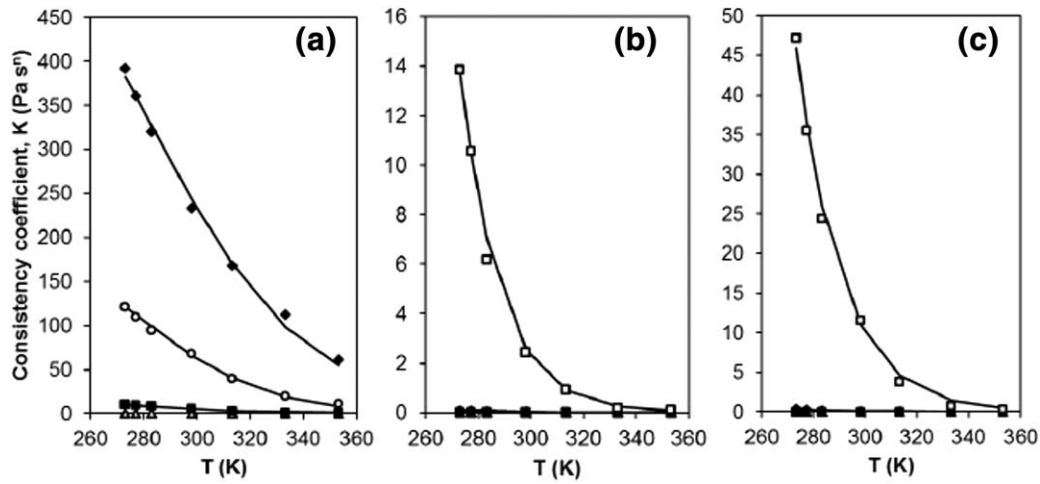
FIGURE 4 Effect of temperature on consistency coefficient of (a) guava, (b) pomelo, and (c) soursop at temperatures of 5°Brix (Δ), 15°Brix (■), 30°Brix (○), 45°Brix (◆), and 70°Brix (□)

2011). Goula and Adamopoulos (2011) mentioned that the fibrous materials influenced the shear-thinning behavior of kiwi fruit juice.

3.2 | Modeling the effect of temperature on the flow behavior of juice concentrates

Results from Tables 5 and 6 on the Arrhenius model for describing the effect of temperature on rheological behavior of fruit juice suggest a poor fit. The values of K should be positive because negative K values results in negative shear rates and will not give a viscosity value (Dealy & Wang, 2013). As all three juices are shear-thinning, it is necessary to make sure the n values remain between 0 and 1. A negative n value is also meaningless and it occurs due to sample slipping out during rheological testing (Fraiha, Biagi, & Ferraz, 2011). In overcoming the limitations of the Arrhenius model, a S-shaped curve, which is the logistic sigmoidal model, was applied to predict the effect of temperature on K and n. Originally, the logistic sigmoidal model is most widely used to describe the growth of population, such as tumor cell growth (Kozusko

& Bourdeau, 2007). The sigmoidal decay model has also been used to evaluate the effect of temperature on lipid solid fat content (Augusto, Soares, et al., 2012). Modeling the current rheological data for juice concentrates using the logistic sigmoidal model, however, did not give a good fit as seen in Tables 5 and 6. A newly proposed model (Equations 9a and 9b) which integrated the Arrhenius and sigmoidal growth models from combined functions of Equation 7a with Equation 8a, and Equation 7b with Equation 8b have provided the highest R^2 ($R^2 = 0.9792-1.0$) and the lowest $RMSE$ ($RMSE = 0.0001-8.2749$) values of all as compared with the Arrhenius model ($R^2 = 0.6243-0.9978$; $RMSE = 0.0002-10.6811$) and the logistic sigmoidal growth models ($R^2 = 0.9440-0.9984$; $RMSE = 0.0001-25.8989$) individually. Statistical analysis in Table 6 also shows that the proposed model is the best fitted model to describe the effect of temperature on n. The negative values of r denote the decay pattern of K by increment of temperature. Activation energy values ranged between 3.23×10^{-5} and 1.20×10^{-2} kJ mol^{-1}, and 7.57×10^{-6} and 9.37×10^{-5} kJ mol^{-1} for T-K and T-n relationships, respectively. The sensitivity of viscosity to
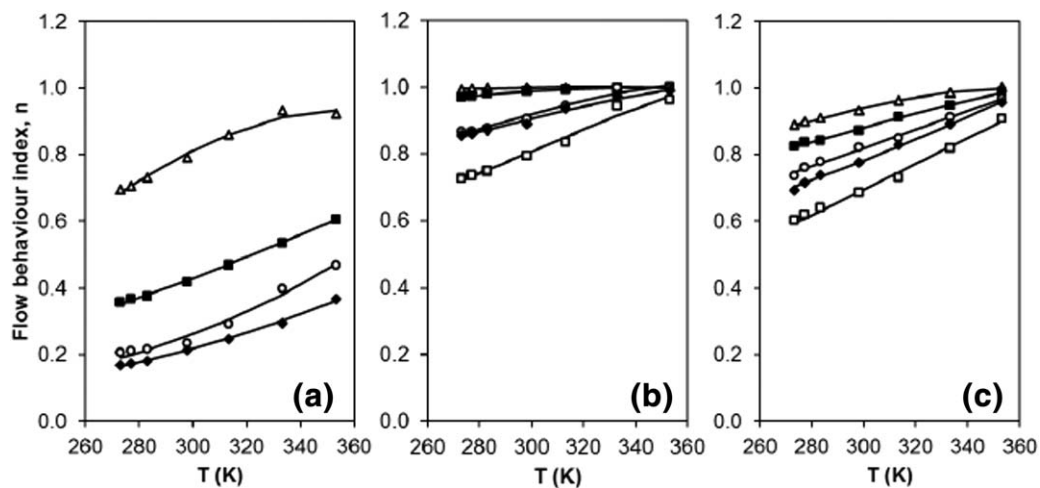

FIGURE 5 Effect of temperature on flow behavior index of (a) guava, (b) pomelo, and (c) soursop at temperatures of 5°Brix (Δ), 15°Brix (■), 30°Brix (○), 45°Brix (◆), and 70°Brix (□)

temperature is shown by its activation energy (Quek et al., 2013). Guava juice concentrate had the lowest range of activation energy as it is less sensitive to a temperature change.

Figures 4 and 5 show a trend of K decaying and growing n with increasing temperature. The K value of fruit juice concentrates reduced at high temperature because heat energy applied has loosen the molecules bonding until they could move fast and random, and leads to less resistance to flow. Figure 4 shows that the guava has the highest range of K, while the pomelo has the lowest range of K. The guava juice concentrate is the most viscous juice compared to the pomelo and soursop. Statistical analysis using ANOVA show that means of K of guava, pomelo, and soursop at different temperatures was significant with $p < .0001$. From DMRT analysis, the highest concentrations at 45°Brix for guava and 70°Brix for the pomelo and soursop lead to a higher K values and this reflected higher juice viscosity. Figure 5 shows that the increment of temperatures caused all the juice concentrates to be more Newtonian. The guava juice concentrates are more shear-thinning, while pomelo juice concentrates are close to Newtonian behavior. The ANOVA results indicate that means of n for all guava, pomelo, and soursop juice concentrates at different concentrations were significantly different with $p < .0001$. From DMRT analysis, the lower means of n at low concentrations of 5°Brix explains the shear-thinning behavior in all juice concentrates.

4 | CONCLUSIONS

The shifting of rheological data to a single reference temperature in developing a master curve model to predict the overall effect of juice concentration on rheological properties of K and n is useful when statistical analysis supports that the data are not significantly different at different temperatures. The master curve models of K or n as function of concentration shows an increasing trend for K and decreasing trend for n. The modeling of K and n with respect to temperature using the Arrhenius and logistic sigmoidal growth models was improved using a new model proposed from the integration of both the Arrhenius and logistic sigmoidal functions. The modeling of fruit juice concentrate properties is potentially useful for the juice processing and equipment industry as it provide avenue to fast, easy, and efficient references on rheological properties for operations and equipment design.

ORCID

Norazlin Abdullah http://orcid.org/0000-0001-8828-8966

REFERENCES

Abdullah, N. (2015). *Optimisation and rheological modelling of thermosonically extracted tropical fruit juice concentrates* (PhD thesis). Universiti Putra Malaysia, Malaysia.

Augusto, P. E. D., Falguera, V., Cristianini, M., & Ibarz, A. (2012). Rheological behavior of tomato juice: Steady-state shear and time-dependent modeling. *Food and Bioprocess Technology*, 5(5), 1715–1723.

Augusto, P. E. D., Soares, B. M. C., Chiu, M. C., & Gonçalves, L. A. G. (2012). Modelling the effect of temperature on the lipid solid fat content (SFC). *Food Research International*, 45(1), 132–135.

Barbana, C., & El-Omri, A. (2012). Viscometric behavior of reconstituted tomato concentrate. *Food and Bioprocess Technology*, 5(1), 209–215.

Bhattacharya, S., & Rastogi, N. K. (1998). Rheological properties of enzyme-treated mango pulp. *Journal of Food Engineering*, 36(3), 249–262.

Chek Zaini, H., Zaiton, H., Zanariah, C. W., & Sakinah, N. (2012). High fiber cookies made from pink guava (Psidium Guajava) decanter/agro waste. Retrieved from http://www.ifr.ac.uk/totalfood2009/Oral%20presentations%20(approved)/Presentation%20-%20Chek%20Zaini%20H.pdf

Chemat, F., Zill, E. H., & Khan, M. K. (2011). Applications of ultrasound in food technology: Processing, preservation and extraction. *Ultrasonics Sonochemistry*, 18(4), 813–835.

Chin, N. L., Tan, M. C., Che Pa, N. F., & Yusof, Y. A. (2013). Method and apparatus for high intensity ultrasonic treatment of baking materials. Google Patents.

Codex. (2005). Codex general standard for fruit juices and nectars (Codex Stan 247–2005, pp. 1–19). Retrieved from http://fao.org

Dak, M., Verma, R. C., & Jaaffrey, S. N. A. (2007). Effect of temperature and concentration on Rheological properties of "Kesar" mango juice. *Journal of Food Engineering*, 80(4), 1011–1015.

Dasgupta, S., & Sarkar, B. (2012). Membrane applications in fruit processing technologies. In: S. Rodrigues & F. A. N. Fernandes (Eds.), *Advances in fruit processing technologies* (p. 101). Boca Raton: CRC Press.

Dealy, J. M., & Wang, J. (2013). Viscosity and normal stress differences. In B. Derby (Ed.), *Melt rheology and its applications in the plastics industry* (pp. 19–47). Dordrecht: Springer.

Economos, C., & Clay, W. D. (1999). Food, nutrition and agriculture: Nutritional and health benefits of citrus fruits. Retrieved from http://www.fao.org/docrep/x2650T/x2650t03.htm

Falguera, V., Vicente, M., Garvín, A., & Ibarz, A. (2013). Flow behavior of clarified pear and apple juices at subzero temperatures. *Journal of Food Processing and Preservation*, 37(2), 133–138.

Fraiha, M., Biagi, J. D., & Ferraz, A. C. O. (2011). Rheological behavior of corn and soy mix as feed ingredients. *Ciência e Tecnologia De Alimentos*, 31(1), 129–134.

Genovese, D. B., & Lozano, J. E. (2001). The effect of hydrocolloids on the stability and viscosity of cloudy apple juices. *Food Hydrocolloids*, 15(1), 1–7.

Goula, A. M., & Adamopoulos, K. G. (2011). Rheological models of kiwifruit juice for processing applications. *Journal of Food Processing and Technology*, 2(1), 1–7.

Jha, S. N., & Gunasekaran, S. (2010). Authentication of sweetness of mango juice using Fourier transform infrared-attenuated total reflection spectroscopy. *Journal of Food Engineering*, 101(3), 337–342.

Juszczak, L., Witczak, M., Fortuna, T., & Solarz, B. (2014). Effect of temperature and soluble solids content on the viscosity of beetroot (Beta vulgaris) juice concentrate. *International Journal of Food Properties*, 13(6), 1364–1372.

Kaya, A., & Sözer, N. (2005). Rheological behaviour of sour pomegranate juice concentrates (Punica granatum L.). *International Journal of Food Science and Technology*, 40(2), 223–227.

Kozusko, F., & Bourdeau, M. (2007). A unified model of sigmoid tumour growth based on cell proliferation and quiescence. *Cell Proliferation*, 40(6), 824–834.

Magerramov, M. A., Abdulagatov, A. I., Azizov, N. D., & Abdulagatov, I. M. (2007). Effect of temperature, concentration, and pressure on the viscosity of pomegranate and pear juice concentrates. *Journal of Food Engineering*, 80(2), 476–489.

Nwokocha, L. M., & Williams, P. A. (2009). New starches: Physicochemical properties of sweetsop (Annona squamosa) and soursop (Anonna muricata) starches. *Carbohydrate Polymers*, 78(3), 462–468.

Pearl, R., & Reed, L. J. (1920). On the rate of growth of the population of the United States since 1790 and its mathematical representation. *Proceedings of the National Academy of Sciences of the United States of America*, 6(6), 275.

Pereira, F. M. V., Carvalho, A. D. S., Cabeça, L. F., & Colnago, L. A. (2013). Classification of intact fresh plums according to sweetness using time-domain nuclear magnetic resonance and chemometrics. *Microchemical Journal*, 108, 14–17.

Quek, M. C., Chin, N. L., & Yusof, Y. A. (2013). Modelling of rheological behaviour of soursop juice concentrates using shear rate-temperature-concentration superposition. *Journal of Food Engineering*, 118(4), 380–386.

Quek, S. Y., Chok, N. K., & Swedlund, P. (2007). The physicochemical properties of spray-dried watermelon powders. *Chemical Engineering and Processing: Process Intensification*, 46(5), 386–392.

Sharma, R., Manikantan, M. R., Ranote, P. S., & Singh, T. (2014). Rheological behavior of litchi juice concentrates during storage. *International Food Research Journal*, 21(3), 1169–1176.

Sharoba, A. M., & Ramadan, M. F. (2011). Rheological behavior and physicochemical characteristics of goldenberry (physalis peruviana) juice as affected by enzymatic treatment. *Journal of Food Processing and Preservation*, 35(2), 201–219.

Steffe, J. F. (1996). *Rheological methods in food processing engineering* (2nd ed.). Michigan, USA: Freeman Press.

Sun-Waterhouse, D., Bekkour, K., Wadhwa, S. S., & Waterhouse, G. I. (2014). Rheological and chemical characterization of smoothie beverages containing high concentrations of fibre and polyphenols from apple. *Food and Bioprocess Technology*, 7(2), 409–423.

Swami Hulle, N. R., Patruni, K., & Rao, P. S. (2014). Rheological properties of aloe vera (aloe barbadensis miller) juice concentrates. *Journal of Food Process Engineering*, 37(4), 375–386.

Vandresen, S., Quadri, M. G. N., de Souza, J. A. R., & Hotza, D. (2009). Temperature effect on the rheological behavior of carrot juices. *Journal of Food Engineering*, 92(3), 269–274.

Yilmaz, M. T., Sert, D., & Demir, M. K. (2010). Rheological properties of tarhana soup enriched with whey concentrate as a function of concentration and temperature. *Journal of Texture Studies*, 41(6), 863–879.